



ΠΑΝΕΠΙΣΤΗΜΙΟ
ΠΑΤΡΩΝ
UNIVERSITY OF PATRAS



ΤΜΗΜΑ ΜΗΧΑΝΙΚΩΝ Η/Υ & ΠΛΗΡΟΦΟΡΙΚΗΣ - ΕΡΓΑΣΤΗΡΙΟ ΑΝΑΓΝΩΡΙΣΗΣ ΠΡΟΤΥΠΩΝ

ΜΟΝΤΕΛΑ ΔΙΑΧΥΣΗΣ ΚΑΡΚΙΝΙΚΩΝ ΟΓΚΩΝ ΕΓΚΕΦΑΛΟΥ

Σ. Λυκοθανάσης, Καθηγητής

Α. Κορφιιάτη, Μηχ/κος Η/Υ & Πληρ/κής
(ΚΕΟ 3)



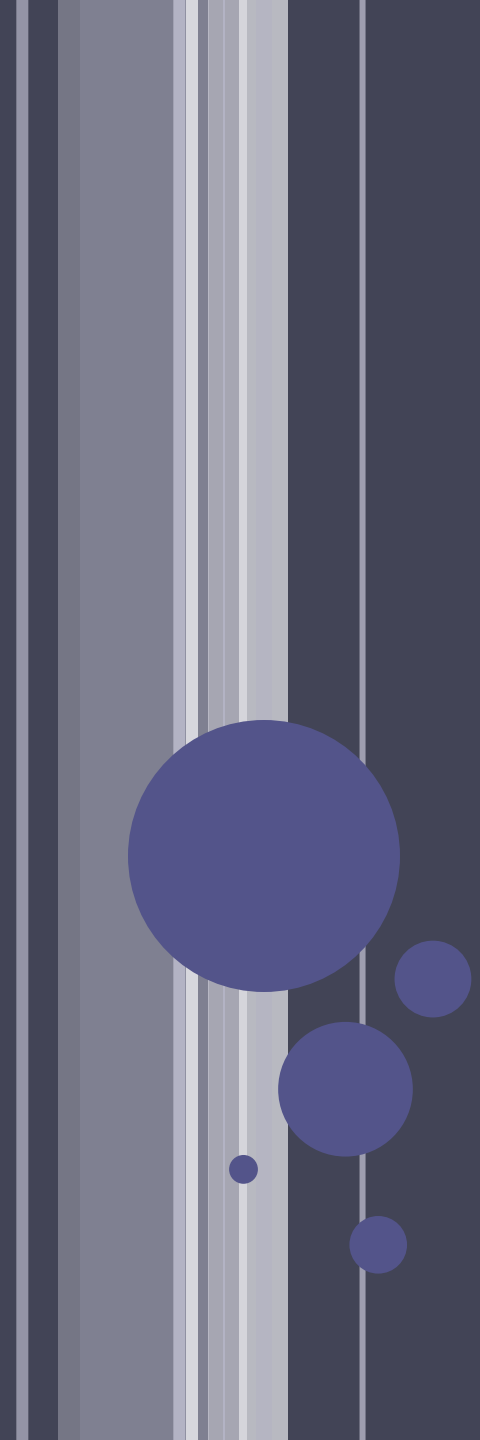
- *This research has been co-financed by the European Union (European Social Fund – ESF) and Greek national funds through the Operational Program "Education and Lifelong Learning" of the National Strategic Reference Framework (NSRF) - Research Funding Program: THALIS. Investing in knowledge society through the European Social Fund.*



THE PROBLEM

Despite continual advances in imaging technology, glioma cells invade far beyond the abnormality shown on clinical imaging (e.g. CT, MRI, or PET) and even beyond gross and microscopic observations at autopsy. The extent is certainly beyond that guiding present-day radiotherapy of gliomas, which targets therapy to only an arbitrary 2 cm beyond the imaged bulk mass of the tumor. Clearly, it is the invasion into the normal-appearing surrounding tissue that is responsible for the tumor recurrence even in those tumors that are radio-sensitive.





**HISTORY OF THE USE OF
MATHEMATICAL MODELING IN THE
STUDY
OF THE PROLIFERATIVE-INVASIVE
GROWTH OF GLIOMAS**

**Hana L.P. Harpold, BS, Ellsworth C. Alvord, Jr., MD,
and Kristin R. Swanson, PhD, The Evolution of
Mathematical Modeling of Glioma Proliferation and
Invasion, J Neuropathol Exp Neurol, Vol. 66, No. 1,
January 2007, pp. 1-9**

EARLY GLIOMA MODEL DEVELOPMENT: GROWTH AND DIFFUSION

- In the early 1990s, Murray's group defined the basic spatio-temporal model, based on the classical definition of cancer, as uncontrolled proliferation of cells with the capacity to invade and metastasize.
- This model was simplified by taking advantage of the fact that gliomas practically never metastasize outside the brain, producing a conservation diffusion equation, written in words in Equation 1.
- rate of change of glioma cell density = net diffusion (motility) of glioma cells in grey and white matter + net proliferation of glioma cell



EARLY GLIOMA MODEL DEVELOPMENT: GROWTH AND DIFFUSION

- Under the assumption of classical gradient-driven Fickian diffusion, this word equation could be quantified mathematically to produce Equation 2.

$$\frac{\partial c}{\partial t} = \nabla(D\nabla c) + \rho c$$

- Equation 2 describes the dynamics of glioma cells where $c(x,t)$ is the concentration of tumor cells at location x and time t . D is the diffusion coefficient representing the net motility of glioma cells and Q represents the net proliferation rate of the glioma cells. The ∇^2 term is the spatial differentiation operator, which is in effect a gradient. Initial conditions for the model were $c(x,0) = f(x)$, where $f(x)$ defined the initial spatial distribution of malignant cells, presumably a point source at the center of tumorigenesis.



BRAIN HETEROGENEITY: ISOTROPIC MIGRATION

- The original analyses of the mathematical model assumed homogenous brain tissue so that the diffusion coefficient D , defining random motility of glioma cells, was constant and uniform throughout the brain.
- Recognizing that the model had to be improved to accommodate the advances in MRI technology that were coming along in parallel, Swanson et al reformulated the model to accept different diffusion rates in grey and white matter.
- This modified model introduced the complex geometry of the brain and presented diffusion (motility) as a function of the spatial variable x to accommodate the observation that glioma cells demonstrate greater motility in white matter than in grey matter.



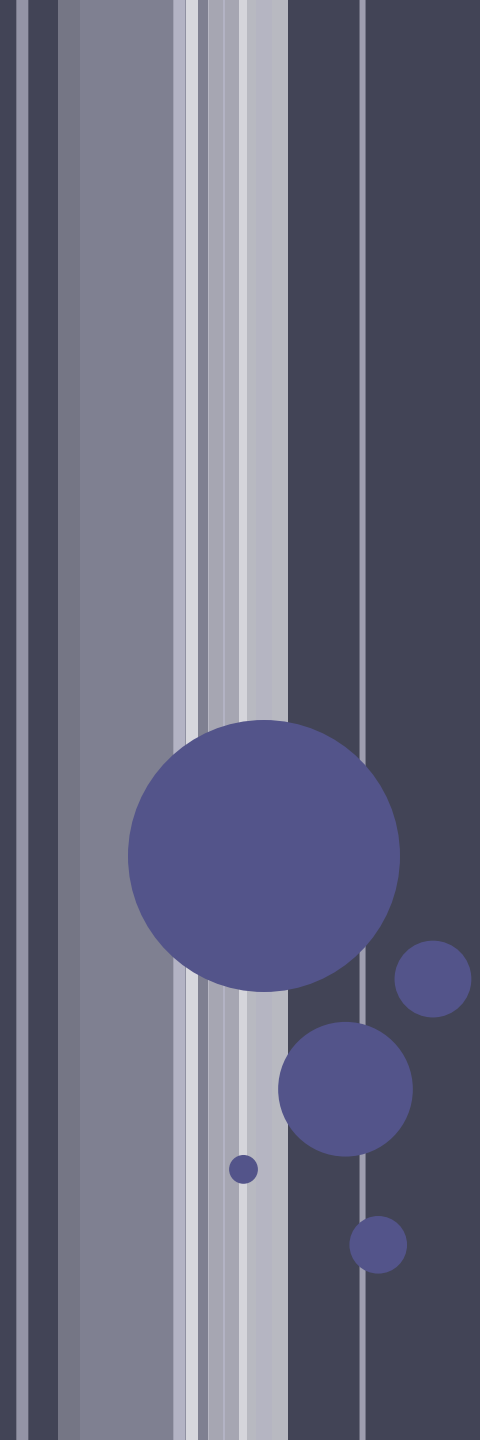
BRAIN HETEROGENEITY: ISOTROPIC MIGRATION

- The original word equation, Equation 1, continued to apply, but the mathematics changed to involve a spatially varying diffusion parameter, $D(\mathbf{x})$, as shown in Equation 3.

$$\frac{\partial c}{\partial t} = \nabla(D(\mathbf{x})\nabla c) + \rho c$$

- $D(\mathbf{x})$ is still defined as the diffusion coefficient defining the net motility of the glioma cells but with $D(\mathbf{x}) = D_G$ or D_W , different constants for \mathbf{x} in grey and white matter, respectively.





AN EXAMPLE: BRAIN TUMOR GROWTH PREDICTION

Md. Rajibul Islam, Norma Alias and Siew Young Ping, An application of PDE to predict brain tumor growth using high performance computing system, daffodil international university journal of science and technology, vol 6, issue 1, july 2011

THE MATHEMATICAL MODEL

$$\frac{\partial u}{\partial t} = -\nabla(Wu) + \nabla(Q\nabla u) + \Gamma - Lu$$

Γ : generation coefficient, L : death/decay coefficient, Q : diffusion coefficient, W : drift velocity field

- The explicit finite-difference method has been used to solve the parabolic equation.
- The finite-differences equations are converted into matrix form.



THE NUMERICAL SOLUTION

- Red Black Gauss Seidel Iteration Method is used to solve the pde
 - division of arrays among local processors.
- The simple Gauss Seidel Iterative method is more appropriate for a sequential program.
- Time execution, speedup, efficiency, effectiveness and temporal performance are the metrics used for comparing parallel and sequential algorithms.



THE HIGH PERFORMANCE COMPUTING SYSTEM

- The cluster contains
 - 6 Intel Pentium IV CPUs (each with a storage of 40GB, speed 1.8MHz and memory 256 MB) and
 - two servers (each with 2 processors, a storage of 40GB, speed AMDAthlon (tm) MP processor 1700++ MHz and memory 1024 MB)
 - connected with internal network Intel 10/100 NIC under RetHat Linux 9.2
- PVM: Parallel Virtual Machine
 - master task
 - worker tasks



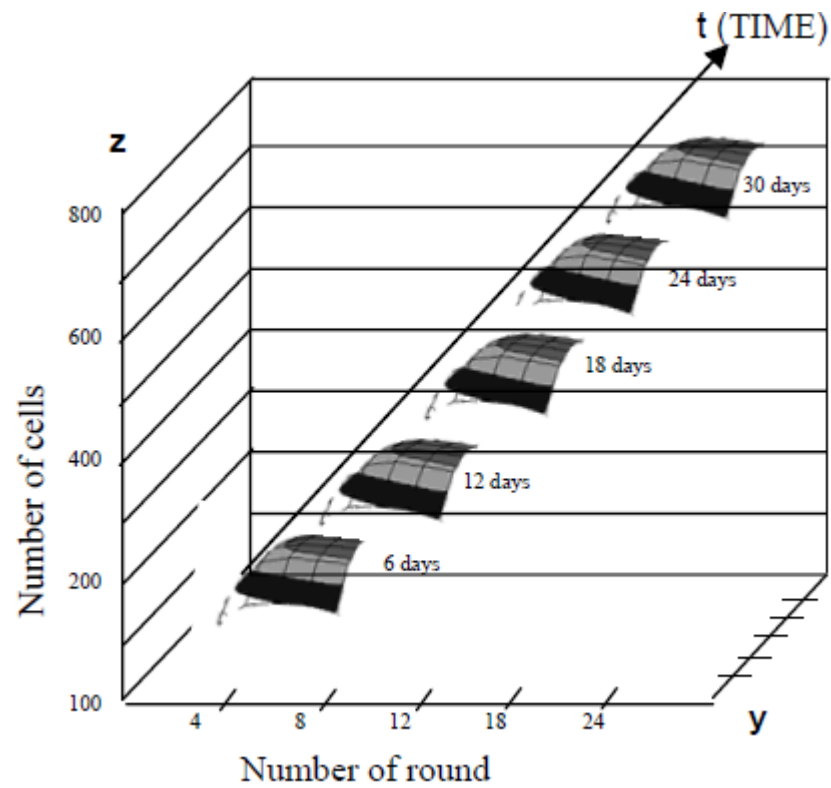
PERFORMANCE ANALYSIS

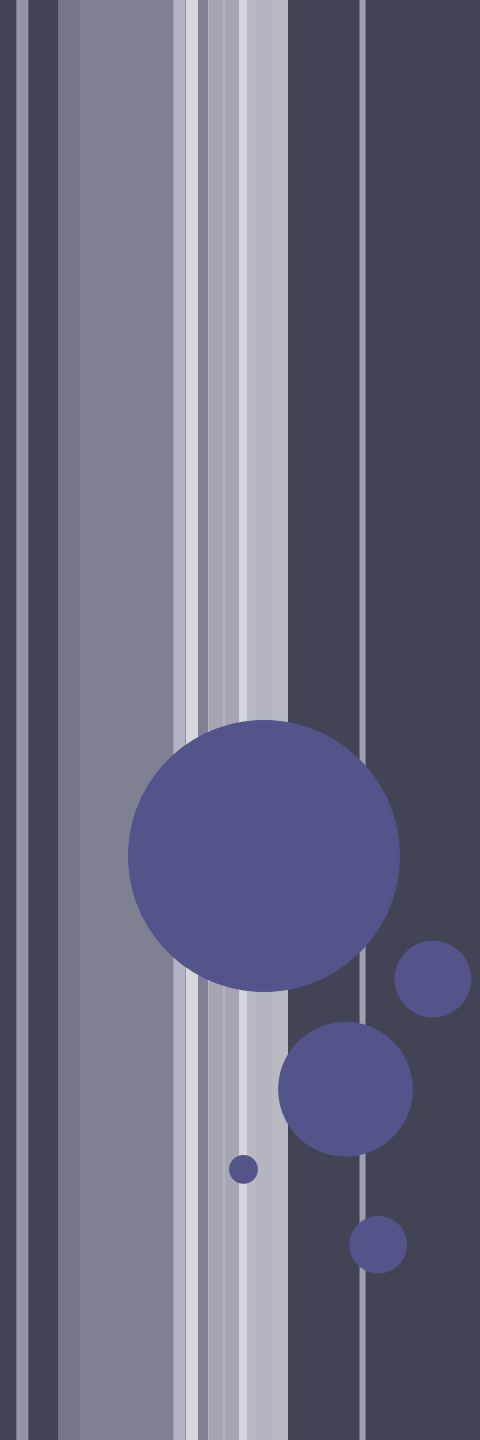
	Red-Black Gauss Seidel with PVM (8 CPU)	Gauss Seidel with Sequence Algorithm (1 CPU)
Time (second)	10.90019	83.153291
Convergence	2.3911e-2	2.3911 e-2
Number of iteration	200	200

Number of processor	Time execution (Second)	Speedup	Efficiency	Effectiveness	Temporal Performance
1	83.153291	1	1	0.012025982	0.012025982
2	41.84082	1.987372	0.993686	0.023749205	0.023900195
3	27.8878808	2.981708	0.993903	0.035639322	0.035857963
4	20.98909	3.961739	0.990435	0.047188072	0.047643800
5	16.9	4.920313	0.984063	0.058228557	0.059171598
6	14.262847	5.830063	0.971677	0.068126448	0.070112229
7	12.362682	6.726153	0.960879	0.077724154	0.080888597
8	10.90019	7.628609	0.953576	0.087482527	0.091741520



RESULTS- EXPANSION RATE OF BRAIN TUMOR



The left side of the slide features a vertical stack of five stripes in varying shades of blue and grey. To the right of these stripes are five circles of different sizes, also in shades of blue, arranged in a descending staircase pattern from top to bottom.

CA²
CELLULAR AUTOMATA MODELS
AND
SELF-ORGANIZED CHAOS
IN CANCER GROWTH

INTRODUCTION 1/2

NOMENCLATURE

CA^2 : Cellular Automaton (CA)
for CAncer Growth



in silico population dynamics
for cancer growth



INTRODUCTION 2/2

ASSUMPTIONS

2-dimensional generalized and probabilistic cellular automata with fixed lattice structure

Each unit (cell) is a 4-state element and at any instance can be found in one of the following conditions: *normal*, *immature cancer*, *matured cancer*, or *dead*.



METHODS 1/5

2-D CA, 4-STATE ELEMENTS

2-dimensional CA with 4-state elements

- *Normal*, denoted by N
- *cancer*, denoted by c (immature phase)
- *cancer, in division phase* denoted by C
- *dead*, denoted by D



METHODS 2/5

CELL TIME CHARACTERISTICS

Each cell is characterized by a triplet of values

- *lifetime*, (T_L) : the total period that a specific cell is alive
- *maturity period* or reproduction age, (T_R) :
time necessary a cell to become “mature enough” to divide and proliferate
- *dissolution time*, (T_D) :
the time necessary the remainings of a dead cell to be exported and the specific grid site to set free



METHODS 3/5

RANDOM INITIALIZATION

The triplet (T_L , T_R , T_D) for each cell are individually defined in a random fashion

Each one of these values is selected randomly from a range of corresponding permitted values with the use of the pseudo-random number generator



METHODS 4/5

CELL DYNAMICS

Local interactions of the CA that are simulating the real inter- and intra-cellular cellular dynamics:

- $N \rightarrow c$ a grid position that was occupied by a normal cell (N) is taken by a new cancer cell (c)
- $c \rightarrow C$ an immature cancer (c) cell gets in the proliferation phase (C)
- $C \rightarrow 2c$ division to two immature cancer cells (2c) of a mature cancer cell (C)
- $c \rightarrow D$ death (D) of an immature cancer cell (c)
- $C \rightarrow D$ death (D) of a mature cancer cell (C)
- $N \rightarrow D$ death (D) of a normal cell (N)
- $D \rightarrow N$ a new normal cell (N) occupies an empty position of a dead cell (D)
- $D \rightarrow c$ a new cancer cell (c) occupies an empty grid position of a dead cell (D)



METHODS 5/5

INITIALIZATION

Initially, (for $t = 0$), the CA is consisted of normal cells, except a user-defined number of cells that turned to cancer cells.

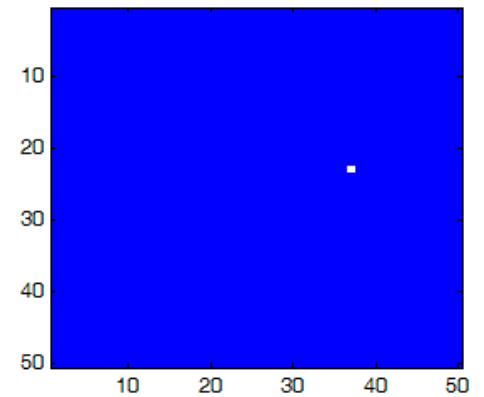
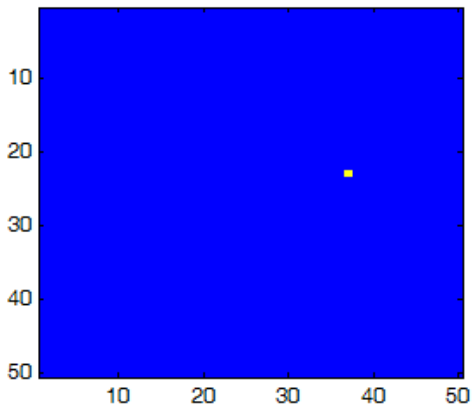
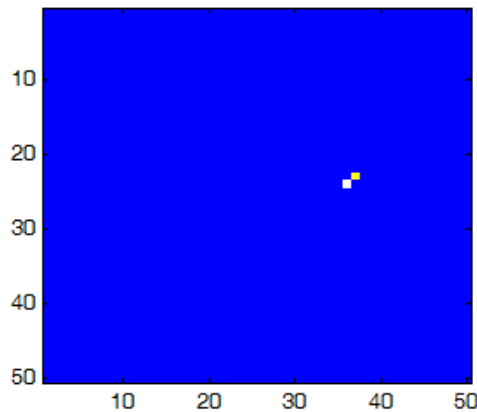
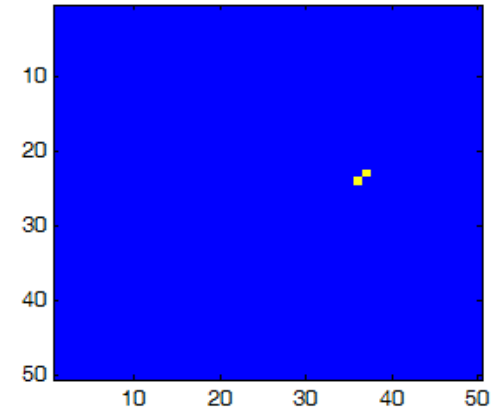
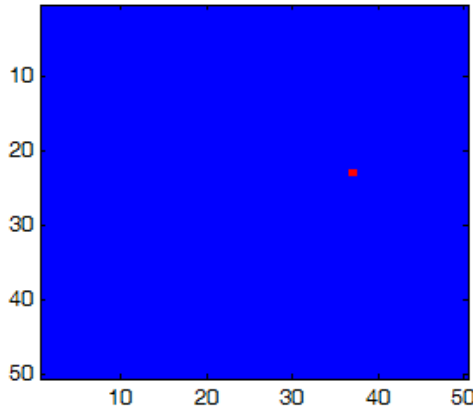
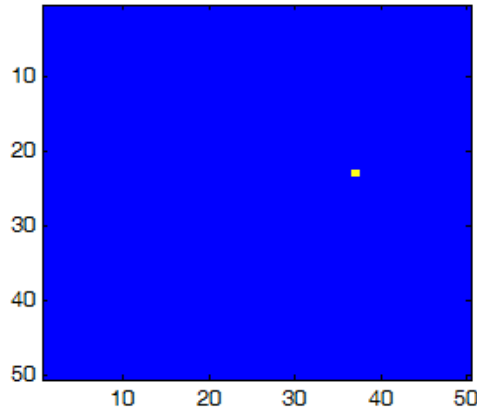
If the number of cancer cells is larger than one for $t = 0$, then a corresponding number of cancer cells subpopulations are evolving simultaneously on the same lattice.

The precise grid position of the cancer cell(s) is (are) randomly selected



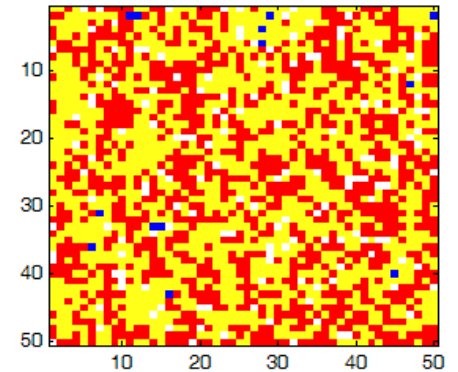
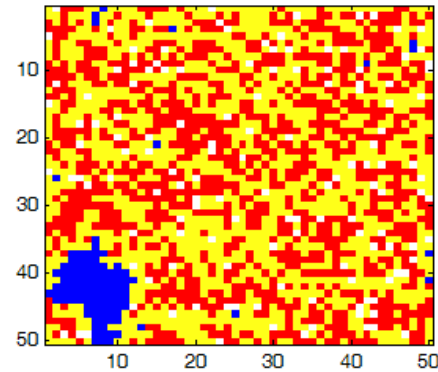
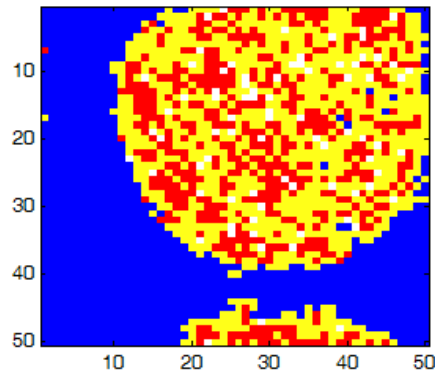
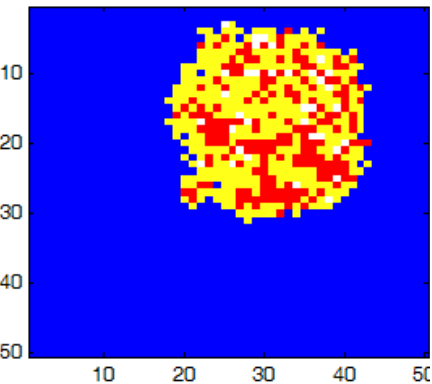
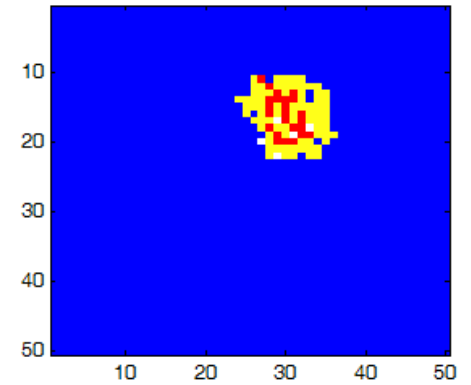
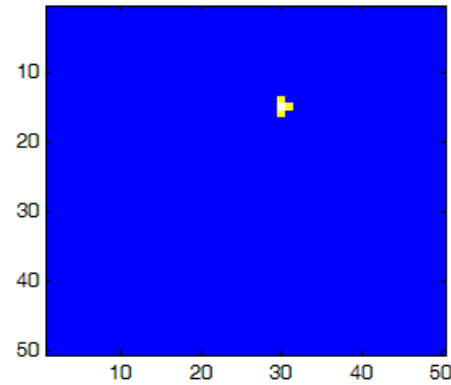
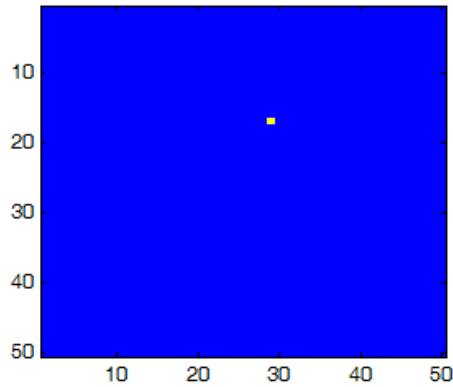
RESULTS 1/4

SINGLE CANCER CELL – NO PROLIFERATION



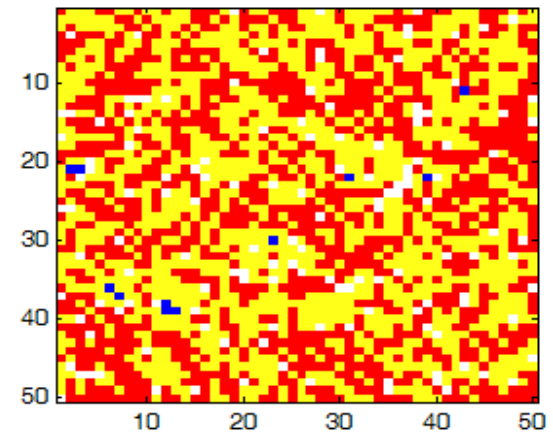
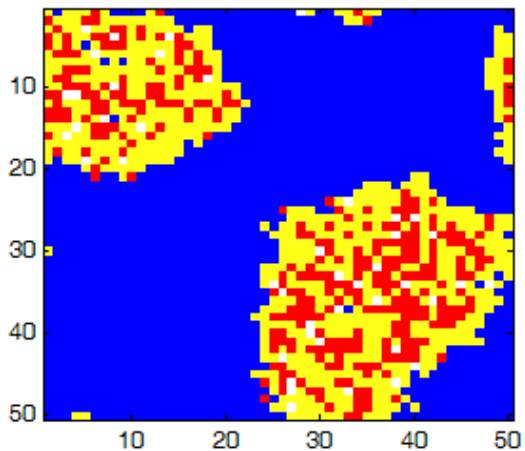
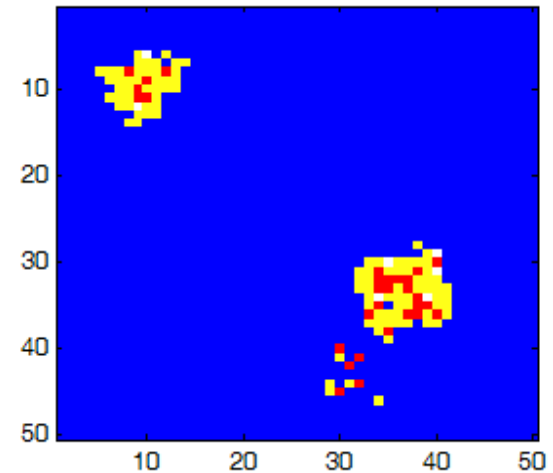
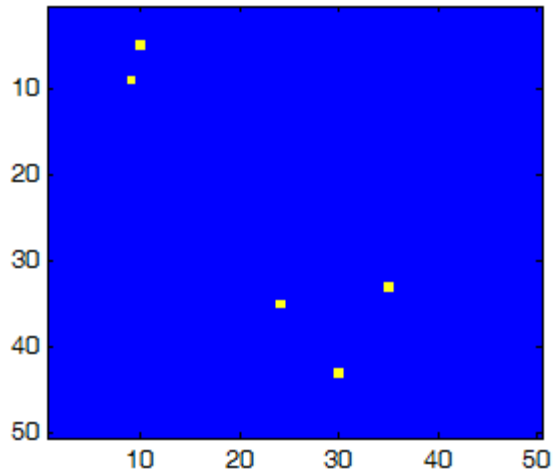
RESULTS 2/4

PROLIFERATION OF A SINGLE CANCER CELL



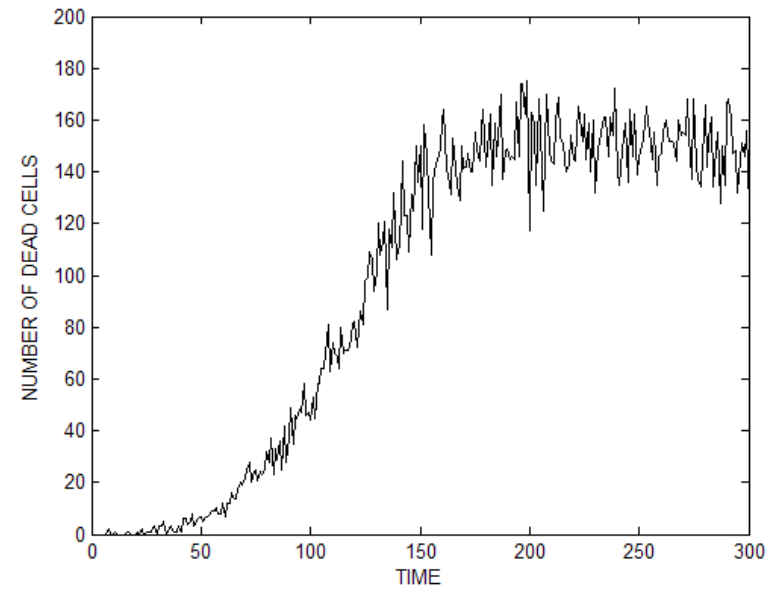
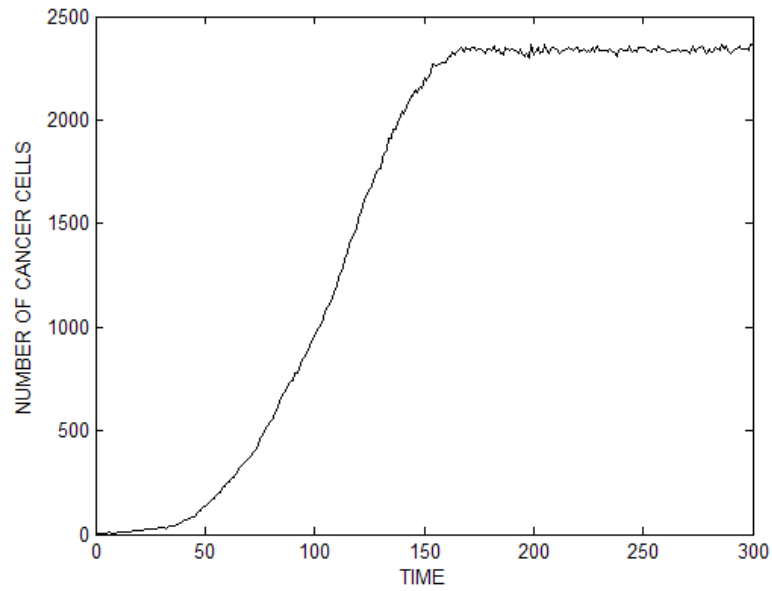
RESULTS 3/4

MULTIFOCAL PROLIFERATION OF 5 SUBPOPULATIONS



RESULTS 4/4

POPULATION EVOLUTION OF CANCER AND DEAD CELLS



DISCUSSION 1/5

REALISTIC BEHAVIOR

The model is able to provide a simple and realistic explanation for the elimination of cancer cells at their early stage of development.

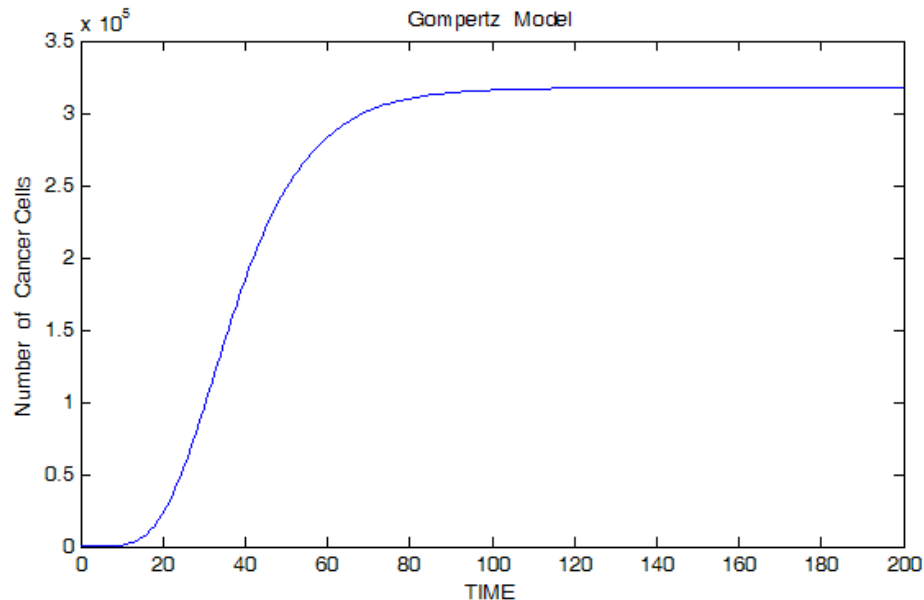
The model is able to provide realistic simulations of cancer proliferation of a single cancer cell.

The model is able to simulate simultaneous growth of multiple subpopulations within the same lattice



DISCUSSION 2/5

GOMPERTZ MODEL



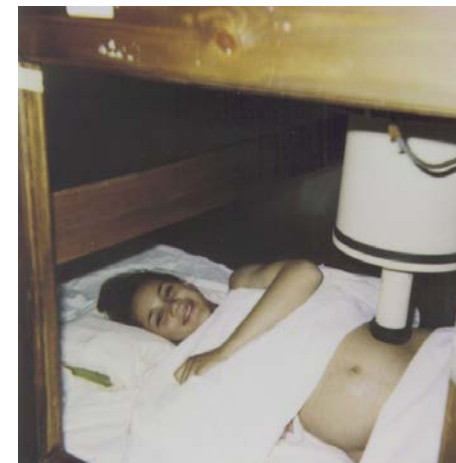
Our findings is in agreement to the Gompertz mathematical model for cancer growth given by:

$$V(t) = V_0 e^{\frac{A}{B}(1-e^{-Bt})}$$



DISCUSSION 3/5

SQUID BIOMAGNETOMETRY - BIOMAGNETIC MEASUREMENTS OF MAGNETIC FIELDS EMITTED BY TUMORS IN BRAIN, BREAST, VAGINA, OVARIES, PROSTATE



DISCUSSION 4/5

CHAOTIC DYNAMICS IN BIOMAGNETIC MEASUREMENTS OF CANCER

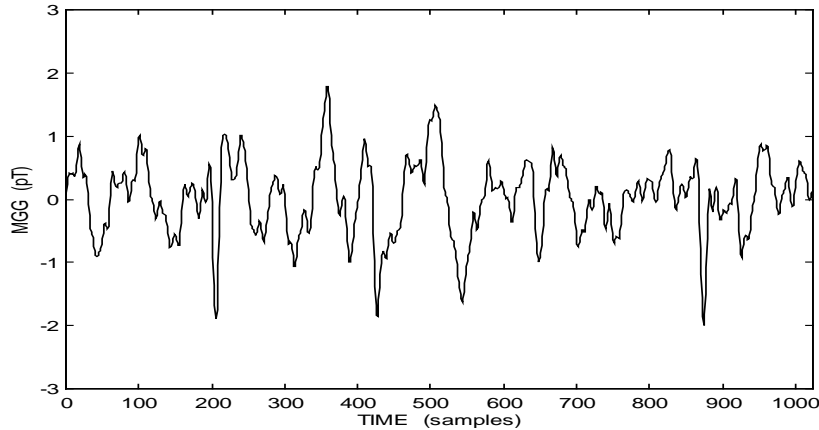


Fig. 1 Biomagnetic signal of MALT carcinoma of 4 sec durations (sampling frequency 256 Hz)

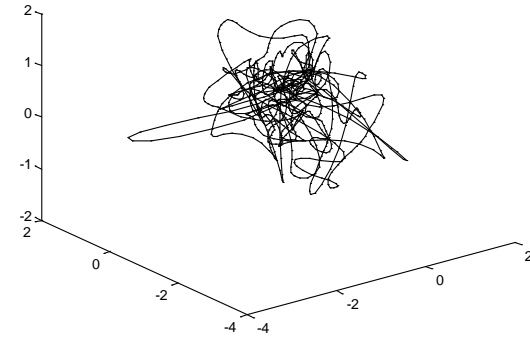


Fig. 2 A 3-D reconstruction of the signal reveals a strange attractor

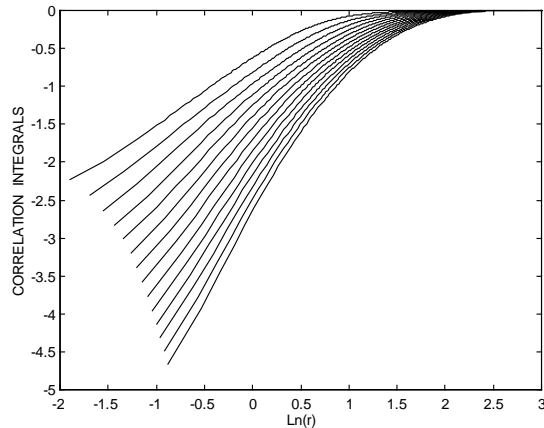


Fig. 3 Correlation integrals

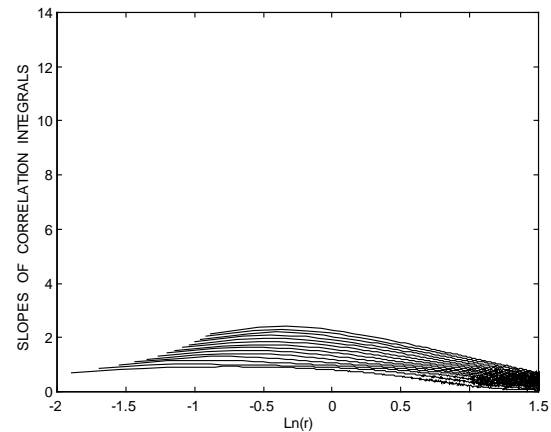


Fig. 4 Slopes of correlation integrals and evidence for convergence to low-dimensional chaotic dynamics



DISCUSSION 5/5

CONCLUSIONS

Our simulation findings provide evidence for emerging non-linear complexity and self-organized chaotic dynamics in cancer growth.

The *hypothesis*, of non-linear dynamics has been proposed for cancer dynamics at sub-cellular and cellular level.

The same *hypothesis* seems to stand at the systemic level as well.

Supported by non-linear analysis of biomagnetic measurements performed *in vivo* for various types of cancer with the use of SQUIDs that indicated the existence of low-dimensional chaotic dynamics in the biomagnetic activity of malignant lesions.



REFERENCES

- P.A. Anninos, A. Kotini, N. Koutlaki, A. Adamopoulos, G. Galazios, & P. Anastasiadis (2000)
Differential diagnosis of breast lesions, by the use of biomagnetic activity and non-linear analysis
Eur. J. of Gyn. Oncol., Vol. XXI, Nr. 6, pp. 591-595.
- P.A. Anninos, A. Kotini, N. Koutlaki, A. Adamopoulos, G. Galazios, P. Anastasiadis (2000)
Differential diagnosis of breast lesions by use of biomagnetic activity and non-linear analysis.
European Journal of Gynaecological Oncology, **XXI(6)**:591-595
- K. Simopoulos, P. Anninos, A. Polychronidis, A. Kotini, A. Adamopoulos, & D. Tamiolakis (2003)
Pre- and postsurgical biomagnetic activity in MALT-type gastric lesions
Acta Radiol., Vol. 44, pp. 1-4.
- P. Anninos, I. Papadopoulos, A. Kotini, & A. Adamopoulos (2003)
Differential diagnosis of prostate lesions with the use of biomagnetic measurements and non-linear analysis
Urol. Res. Vol. 31, pp. 32-36.
- P. Antoniou, P. Anninos, H. Piperidou, A. Adamopoulos, A. Kotini, M. Koukourakis, E. Sivridis (2004)
Non-linear analysis of magnetoencephalographic signals as a tool for assessing malignant lesions of the brain: first results
Brain Topography, **17(2)**:117-123

